

Research Paper

Finding optimal conductive additive content to enhance the performance of coated sorption beds: An experimental study

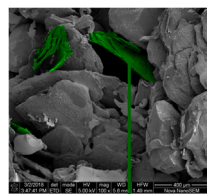
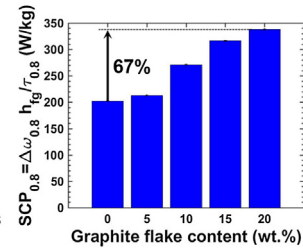
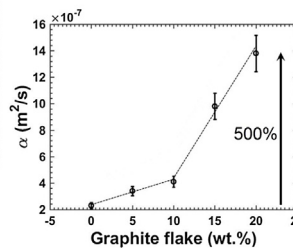
H. Bahrehmand, M. Khajepour, M. Bahrami*

Laboratory for Alternative Energy Conversion (LAEC), School of Mechatronic Systems Engineering, Simon Fraser University, Surrey, BC V3T 0A3, Canada

HIGHLIGHTS

- Transient measurement using custom-built gravimetric large pressure jump test bed.
- Graphite flake additives in CaCl_2 -silica gel composite sorbents.
- Enhancement of sorbent thermal diffusivity by 500% with 20 wt% graphite flake.
- 65% increase in SCP and 17% increase in COP with 20 wt% graphite flake.

GRAPHICAL ABSTRACT

Graphite flake in CaCl_2 -silica gel composite

ARTICLE INFO

Keywords:

Sorption cooling system
Graphite flakes
Heat transfer enhancement
Specific cooling power
Coefficient of performance
Thermal diffusivity

ABSTRACT

Adding natural graphite flakes to sorbents of sorption cooling systems can significantly enhance the overall thermal diffusivity, while reducing the active material and increasing mass transfer resistance. To find an optimum compromise between these counteracting trends, the sorption performance of CaCl_2 -silica gel composite sorbents with 0–20 wt% graphite flakes content are tested using a custom-built gravimetric large pressure jump (G-LPJ) test bed. It is observed that in the early stages of sorption, i.e. sorption time less than 20 min, graphite flakes additives increase the specific cooling power (SCP) (from 365 to 604 W/kg for 5 min sorption time, a 65% increase) and coefficient of performance (COP) (from 0.46 to 0.54 for 5 min sorption time, a 17% increase) due to the enhanced sorbent thermal diffusivity (from 0.23 to 1.38 m^2/s , a 500% increase). Over time, as the sorbent approaches equilibrium, the performance enhancement deteriorates by increasing graphite flakes content since there is less active material in the composite. Furthermore, adding 20 wt% graphite flakes to the composite sorbent has led to a 67% increase in $\text{SCP}_{0.8}$ (SCP when the sorbent reaches 80% of equilibrium).

1. Introduction

Vapor compression refrigeration systems (VCR) consume approximately 15% of global electrical energy and use environmentally harmful refrigerants, i.e. hydrofluorocarbon [1–3]. Moreover, vehicle air conditioning (A/C) systems, VCR, significantly increases fuel consumption, in fact vehicle A/C is the second largest consumer of fossil energy after vehicle propulsion [4]. As an alternative to VCR, sorption

cooling systems are eco-friendly since they employ natural working fluids, i.e. water vapor, as refrigerants [5,6]. Furthermore, sorption cooling systems utilize materials with low regeneration temperatures and can be powered by low-grade heat sources, i.e. temperature sources around 80 °C, including solar thermal energy and industrial waste heat [5]. In addition, in an internal combustion engine (ICE) vehicle, almost 70% of total fuel energy is dissipated through the ICE coolant and exhaust gas in the form of waste heat [7], which can be used to regenerate

* Corresponding Author at: School of Mechatronic Systems Engineering, Simon Fraser University, 250-13450 102 Avenue, Surrey, BC V3T 0A3, Canada.
E-mail addresses: sbahrehm@sfu.ca (H. Bahrehmand), mkhajepour@sfu.ca (M. Khajepour), mbahrami@sfu.ca (M. Bahrami).

Nomenclature		sorber)	
c	specific heat capacity, J/kg K	<i>Subscripts</i>	
h_{ads}	enthalpy of adsorption, J/kg	evap	evaporator/evaporative
h_{fg}	enthalpy of evaporation, J/kg	eq	equilibrium
p	pressure, Pa	sorb	sorbent
p_0	saturation pressure, Pa	sorp	sorption
Q	energy, J	<i>Abbreviations</i>	
T	temperature, K	COP	coefficient of performance
t	time (s)	HEX	heat exchanger
<i>Greek symbols</i>		G-LPJ	gravimetric large pressure jump
α	thermal diffusivity, m^2/s	SCP	specific cooling power
τ	cycle time, s	TCR	thermal contact resistance
φ	graphite flake content in the sorbent (g H_2O/g dry		

the sorbent and generate cooling for air conditioning.

However, commercialization of sorption cooling systems is limited by fundamental challenges, including low specific cooling power (SCP) and low coefficient of performance (COP) due to poor heat transfer between the sorber bed heat exchanger (HEX) and the sorbent material [8–10]. Sorber beds need to be cooled/heated during the sorption/desorption process to maintain efficient uptake. As such, improving heat transfer characteristics of the sorbent and HEX are crucially important to the overall performance of the sorption systems. It has been shown in our previous studies [11,12] that the sorbent thermal diffusivity is the main limiting factor in the heat transfer from the sorbent to the heat transfer fluid through the heat exchanger. Hence, developing composite sorbents with higher thermal conductivity and lower specific heat and density (low thermal inertia) can enhance the overall performance of adsorbent beds [13,14]. Addition of high thermal diffusivity material can form higher conductivity paths by filling up the pores in the microstructure of the adsorbent particles to increase the overall thermal diffusivity. However, in general, these additives decrease the active material fraction and increase the vapor transport resistance [15]. Moreover, many microporous adsorbents have open pore structures and high total pore volumes [16]. As a result, significant improvements in thermal diffusivity of microporous adsorbent materials have been limited to high additive fractions (> wt%), compromising the total adsorption capacity.

Demir et al. [17] used metallic particle additives to enhance heat transfer rate through an unconsolidated adsorbent bed. Silica gel with metallic additives of copper, brass and aluminum (strips with 0.1 mm thickness, 2 mm width and 10 mm length) up to 15% in mass basis has been investigated. They noticed that the addition of 15 wt% of aluminum pieces to silica gel enhanced thermal conductivity of a pure silica gel bed by 242% (from 0.106 to 0.363 W/m K). They did not study the effects of the additives on the overall performance of

adsorption cooling systems. Askalany et al. [18] studied the effect of using metallic additives on thermal conductivity of granular activated carbon (1–2 mm). Fillings of iron, copper and aluminum at different mass concentrations ranging from 10 to 30% have been studied. They reported that thermal conductivity increased with an increase in metallic additives concentrations. However, metallic additives are not suitable for corrosive sorbents such as salt/porous matrix composites. Therefore, graphite particles/additives might be a better candidate when a corrosive sorbent is used. Compared to most metals, graphite has higher intrinsic thermal conductivity, lower molecular weight and excellent stability at high working temperatures [15], and therefore can be a suitable additive to enhance the sorbent thermal diffusivity.

Graphite is by far the most studied additive when developing composite sorbents with the purpose of enhancing thermal conductivity [19]. When comparing different host matrices or/and additives, graphite presents the highest conductivity values [20]. For instance, Mauran et al. [21] reported thermal conductivities of about 10–40 $W(m\cdot K)^{-1}$ for a $CaCl_2$ -expanded natural graphite (ENG) composite.

Summary of the existing studies on the effect of graphite additives on the heat and mass transfer of sorbent materials and the gaps in the open literature are presented in Table 1. It can be seen that some of the studies did not report the water uptake, whereas the effect of graphite additive on water uptake is crucial in sorption performance and should be investigated. The majority of the studies that reported the water uptake, investigated the equilibrium uptake using small-scale measurements, i.e. where sorbents in the order of milligrams are tested, which reaches equilibrium quickly because of the low heat and mass transfer resistances. However, due to the transient behavior of sorber beds and relatively larger heat and mass transfer resistances in sorption chillers, the sorbent does not reach equilibrium to become fully saturated/dried during sorption/desorption in large-scale sorption cooling systems [22]. Hence, in this paper, a gravimetric large pressure jump

Table 1

Summary of the existing studies on the effect of graphite additive on heat and mass transfer of the sorbent and the gap in the research.

Ref. No.	Sorbent	Thermally conductive additive	Increase in thermal conductivity $W(m\cdot K)^{-1}$	Uptake ($g\cdot g^{-1}$)	Gap in the research
[23]	Packed bed zeolite	Expanded graphite	0.09 to 10	Not reported	Uptake not reported.
[16]	4A-zeolite-based composite	Graphite (40%)	0.1 to 0.35	Equilibrium uptake decreased from 0.23 to 0.13	Equilibrium uptake reported.
[24]	$CaCl_2$	Expanded graphite	Up to 9.2	Not reported	Uptake not reported
[25]	$CaCl_2$ and silica gel	Graphite flakes (20%)	0.57 to 0.78	Equilibrium uptake decreased from 0.32 to 0.15	Equilibrium uptake reported
[26]	silica gel	Expanded graphite (40%)	Up to 19	Transient uptake increased	Graphite weight was not included in calculations
[27]	silica gel	Expanded natural graphite treated with sulfuric acid (ENG-TSA)	Up to 20	Transient uptake increased	Graphite weight was not included in calculations

(G-LPJ) test bed was custom-built to study the transient behavior of water uptake using large-scale measurements.

Furthermore, it can be seen in Table 1 that the studies, in which the transient behavior of the uptake were investigated, reported the sorption capacity per mass of “active material”, while the additive mass, as part of the composite sorbent, should be included in the calculations of water uptake. By including the graphite mass in the denominator of water uptake, the transient water uptake reported would decrease because of high concentrations of graphite in the sorbent (as high as 50%). For example, it can be seen in Table 1 that some of the studies reported very high thermal conductivities. Nonetheless, high concentrations of ENG were used, which considerably reduces the sorption capacity

In this paper, a number of CaCl₂-silica gel composite sorbents with 0–20 wt% graphite flake contents are prepared and tested in our custom-made G-LPJ test bed to study the counteracting effect of graphite additive on the transient heat and mass transfer performance of sorption cooling systems. Our water uptake calculations include the graphite mass.

2. Experimental study

2.1. Sample preparation

Polyvinylpyrrolidone (PVP40) binder (40,000 MW, Amresco Inc.) was dissolved in water; subsequently, CaCl₂ and silica gel (SiliaFlash® B150, Silicycle, Inc., Quebec, Canada) and graphite flakes (consisting of both 150 μm fine particles and thin flakes up to 1.3 mm long, Sigma-Aldrich) were added to the aqueous solution. The composition and total mass of the sorbent composites prepared in this study are presented in Table 2. The slurry composites were coated on graphite sheets and oven dried at 70 °C and then 180 °C, each for 1 h. Fig. 1 shows the composite sorbent with 20 wt% graphite flake content coated on a graphite sheet. Dry sorbent mass was measured using an analytical balance (OHAUS AX124) with the accuracy of 0.0001 g and sorbent thickness was measured using a digital caliper (Mastercraft 58-6800-4) with the accuracy of 0.01 mm.

2.2. Thermal diffusivity measurements

Thermal diffusivity of composite sorbents with different graphite flake contents was measured using a transient plane source, hot disk thermal constants analyzer, as per ISO 22007-2 [28] (TPS 2500S, ThermTest Inc., Fredericton, Canada), available in our lab. Details of TPS testing can be found elsewhere [25]. The tests were performed in a temperature and humidity-controlled chamber. The thermal diffusivity of the composite sorbents was tested five times to ensure repeatability and a standard deviation of 10% was observed. The samples were tested at 10% and 40% relative humidity at 40 °C to be consistent with G-LPJ measurements in Section 2.4. The averaged values of thermal diffusivity versus graphite flake are plotted in Fig. 2. It can be seen that addition of 20 wt% graphite flakes to the composite sorbent enhances the thermal diffusivity by 483%. Such enhancement in thermal diffusivity is attributed to the dispersion of graphite flakes through the composite, and hence, the formation of conductive networks within the sorbent matrix. Moreover, we noticed a more pronounced increase in thermal diffusivity for samples with more than 10 wt% graphite flakes. This “hockey stick” behavior can be explained by thermal percolation threshold [29]. Percolation threshold determines the probability that fillers/additives within a medium are sufficiently connected to form a conductive network [30]. Therefore, when certain volume is available in the composite matrix, the graphite flakes should be added up to the amount that is enough for making a conductive network within the composite to increase the thermal conductivity and diffusivity [29].

2.3. Material characterization

The composite microstructure was imaged using a scanning electron microscope (FEL/Aspex-Explorer) at room temperature. Fig. 3 shows the dispersion of graphite flakes (demarcated in green) in between CaCl₂, Silica gel particles and binder in the composite. The SEM images reveal that, graphite flakes with the size of ~500 × 30 μm distributed in the composite are held by the polymer binder and form a thermally-conductive network, which allows a better heat transfer through the composite. According to percolation theory [29–31] discussed in Section 2.2, it is important to consider the amount of the graphite flake relative to the available volume in the composite for their dispersion for percolation to occur, which increases the thermal conductivity significantly.

Water sorption isotherms of our sorbent composites are obtained using an IGA-002 thermogravimetric sorption analyzer (TGA) (Hidden Isochema) and shown in Fig. 4. Sorbent material was placed on the sample cell, which was held by a microbalance to measure the mass changes of the sorbent, while the temperature and pressure were controlled. The mass changes of the sorbent were collected in the range of 0.04–2.84 kPa with the pressure step of 0.2 kPa at 25 °C. As expected, the composites with higher contents of conductive additives showed less water uptake as they had less active sorbent material content. More details regarding the TGA measurements can be found elsewhere [25]. The pressure range, where the G-LPJ measurements were performed, is demarcated on Fig. 4. More details on our G-LPJ tests can be found in Section 2.4.

Dubinin–Astakov equation (D–A) [9,32] was fitted to the equilibrium uptake data using a MATLAB code and the following correlation was obtained with an R² of 0.9954.

$$\omega_{eq} = (1-\varphi) \left(9.01 \exp \left(-0.5485 \left(T \ln \left(\frac{p_0}{p} \right) \right)^{0.2850} \right) \right) \quad (1)$$

where φ is the ratio of graphite weight to the total composite weight and T is the sorbent temperature.

2.4. Experimental test-bed and measurements

A gravimetric large pressure jump (G-LPJ) test bed was custom-built in our lab to investigate the heat and mass transfer performance of sorbent materials, heat exchangers and fin arrangements, as well as various sorbent coatings. Sorbent materials consisting of CaCl₂, silica gel B150, PVP-40, and 0–20 wt% graphite flakes were coated on 1.8 mm thick graphite sheets (with the density of 1,318 kg/m³) and bolted to a copper heat exchanger as shown in Fig. 5. Heat transfer fluid was pumped through the copper heat exchanger to maintain its temperature constant at 39 °C. The sorber bed and the copper heat exchanger were placed inside a vacuum chamber which was connected to a capillary-assisted evaporator/condenser whose temperature was changed between 1 °C and 20 °C for desorption and adsorption, respectively. The whole test bed was vacuumed for 6 h using a vacuum pump to dry the sorbent material. The vacuum chamber was placed on

Table 2

Compositions, total mass, and measured thermal diffusivity of the sorbent composite samples.

No.	Silica gel (wt %)	CaCl ₂ (wt%)	PVP40 (wt%)	Graphite flake (wt%)	Dry mass (g)	Coating Thickness (mm)
1	45.0	45.0	10	0	18.8068	5.15
2	42.5	42.5	10	5	18.7018	5.12
3	40.0	40.0	10	10	18.7841	5.08
4	37.5	37.5	10	15	18.6930	5.09
5	35.0	35.0	10	20	18.8815	5.06

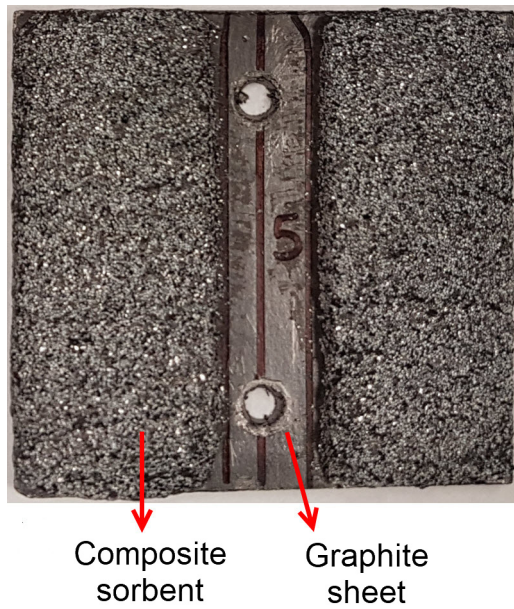


Fig. 1. The composite sorbent with 20 wt% graphite flake content coated on graphite sheet substrates.

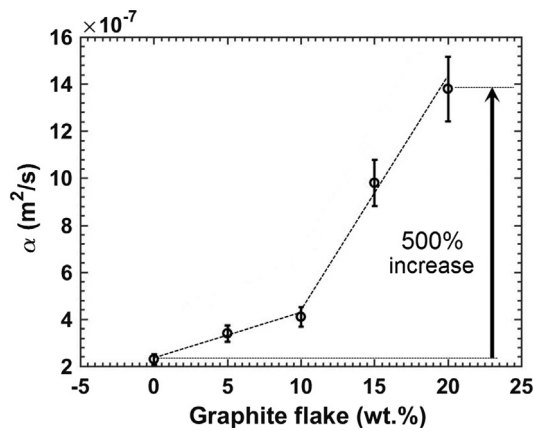


Fig. 2. Thermal diffusivity of our sample sorbent composite versus graphite flake content.

a precision balance (ML4002E, Mettler Toledo) with an accuracy of 0.01 g to measure the mass of the sorbate uptake. Five K-type

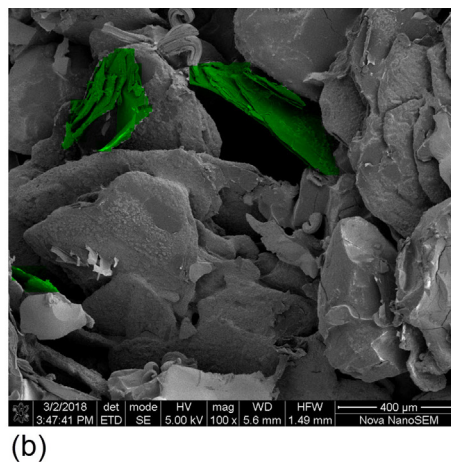
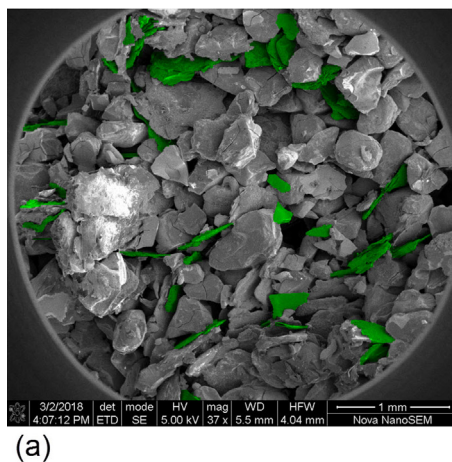


Fig. 3. SEM images of composite sorbent with 20 wt% graphite flake content (graphite flakes demarcated in green).

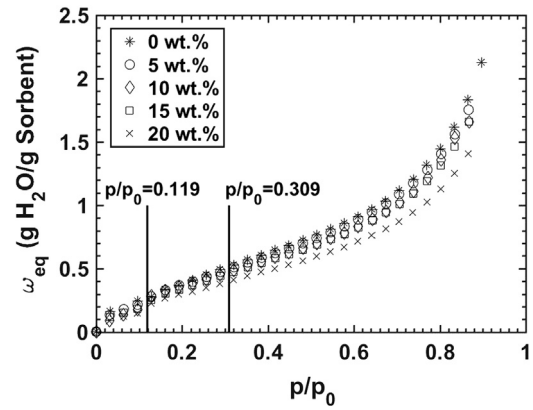


Fig. 4. Isotherms of the composite sorbents with different graphite flake contents.

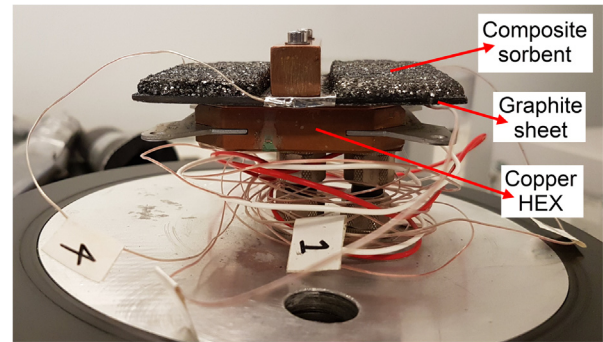


Fig. 5. Graphite coated composite sorbent connected to the copper heat exchanger.

thermocouples with an accuracy of 1.1 °C were passed via a feed-through in the vacuum chamber to measure the sorbent temperature. The pressure of the sorber bed and the evaporator was measured using 722B Baratron pressure transducer (MKS instruments) with the accuracy of 0.5%. The instruments were interfaced with a PC through a data acquisition system and in-house software built in the LabVIEW environment. A schematic diagram of our G-LPJ test bed is shown in Fig. 6.

2.5. Uncertainty analysis

Specific cooling power (SCP) is defined as the ratio of evaporative

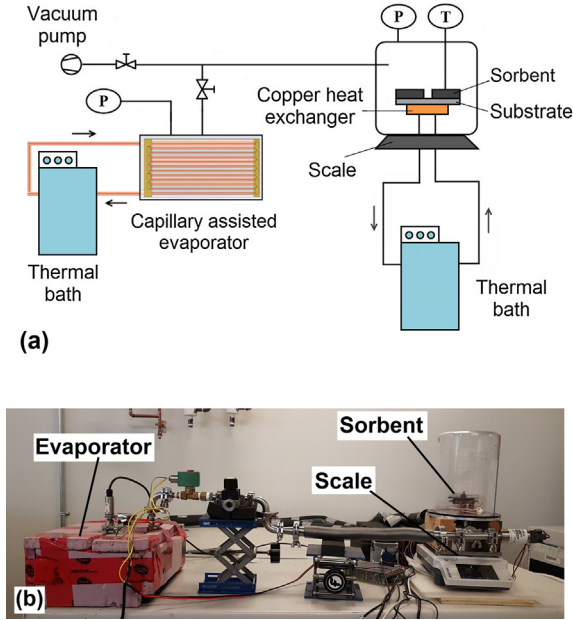


Fig. 6. (a) Schematic diagram and (b) picture of the G-LPJ test bed, thermal baths are not shown in (b).

cooling energy to the product of cycle time and dry sorbent mass, Eq. (2).

$$SCP = \frac{Q_{evap}}{m_{sorb} \tau_{cycle}} = \frac{\Delta\omega h_{fg@T_{evap}}}{\tau_{cycle}} \quad (2)$$

The uncertainty in SCP calculation is obtained based on the method proposed by Moffat [33] as follows.

$$\frac{\delta SCP}{SCP} = \frac{\delta \Delta\omega}{\Delta\omega} = \frac{\sqrt{2} \delta\omega}{\Delta\omega} \quad (3)$$

$$\omega = \frac{m_{sorbate}}{m_{sorbent}} \quad (4)$$

$$\frac{\delta\omega}{\omega} = \sqrt{\left(\frac{\delta m_{sorbate}}{m_{sorbate}}\right)^2 + \left(\frac{\delta m_{sorbent}}{m_{sorbent}}\right)^2} \cong \left(\frac{\delta m_{sorbate}}{m_{sorbate}}\right) = \frac{0.01g}{m_{sorbate}} \quad (5)$$

Sorbent mass was measured using an analytical balance (OHAUS AX124) with the accuracy of 0.0001 g, whereas the sorbate mass change was measured by precision balance (ML4002E, Mettler Toledo) with the accuracy of 0.01 g. Therefore, the sorbent mass uncertainty was negligible compared to that of sorbate.

Finally, the uncertainty in SCP calculation is obtained using Eq. (7). Substituting the sorbent mass and differential sorbate uptake in Eq. (7), the SCP uncertainty is estimated to be between 0.24 and 3.83% for different samples and cycle times.

$$\delta\omega = \frac{0.01g}{m_{sorbent}} \quad (6)$$

$$\frac{\delta SCP}{SCP} = \frac{0.01 \sqrt{2}}{m_{sorbent} \Delta\omega} \quad (7)$$

Coefficient of performance (COP) is defined as the ratio of evaporative cooling energy to the input energy, Eq. (8).

$$COP = \frac{Q_{evap}}{Q_{input}} = \frac{m_{sorb} \int_{ads} \frac{d\omega}{dt} h_{fg} dt}{\int_{des} \left((m_{sorb} (c_{p,s} + \omega c_{p,w}) + m_{HEX} c_{p,HEX}) \frac{dT}{dt} - m_{sorb} \frac{d\omega}{dt} h_{ads} \right) dt} \quad (8)$$

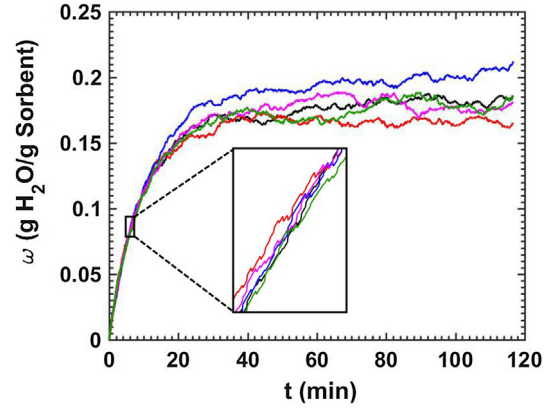


Fig. 7. Five water uptake measurements of the sorbent with 20 wt% graphite flakes.

The main uncertainty in COP calculation is due to the uptake measurement and can be calculated by Eq. (9). The COP uncertainty is estimated to be between 0.48 and 7.66% for different samples and cycle times.

$$\frac{\delta COP}{COP} = \frac{\sqrt{2} \delta \Delta\omega}{\Delta\omega} = \frac{2\delta\omega}{\Delta\omega} \quad (9)$$

3. Results and discussion

Due to the small vibrations of the hose connected to the sorber bed in our G-LPJ test bed, see Fig. 6, a very small shift occurs in the mass measurement within short time intervals. When all these small shifts get accumulated over time, they result in larger shifts. Nonetheless, considering the randomness of these shifts, the error decreases as more tests are done. Hence, each measurement was conducted five times and the maximum standard deviation of water uptake was observed to be 7%. As an example, five water uptake measurements of the sorbent with 20 wt% graphite flakes are plotted in Fig. 7.

Variation of evaporator/condenser and sorber bed pressure, sorbent temperature and water uptake versus time are shown in Figs. 8-10. As shown in Fig. 8, during the sorption process, the evaporator and sorber bed pressure is 2.34 and 2.16 kPa, and during the desorption process, the condenser and sorber bed pressure is 0.65 and 0.83 kPa, respectively. These pressure values of the sorber bed and its temperature, i.e. 39 °C, correspond to $p/p_0 = 0.309$ and 0.119 for sorption and desorption processes, respectively (Fig. 4). Moreover, the large pressure jump at the beginning of each sorption and desorption process can be observed. As shown in Fig. 9, at the beginning of de/adsorption process, the sorbent temperature de/increases rapidly due to endo/exothermic

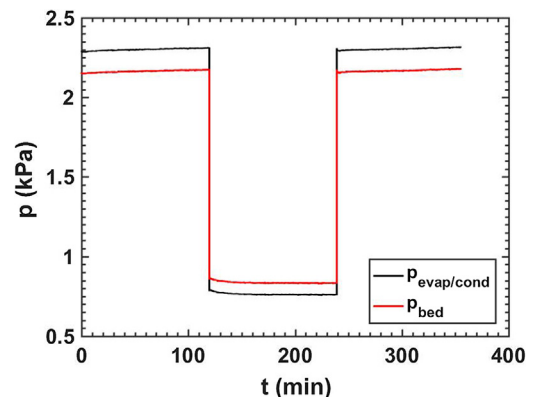


Fig. 8. Variation of evaporator/condenser and sorber bed pressure with time, data collected in our G-LPJ test bed.

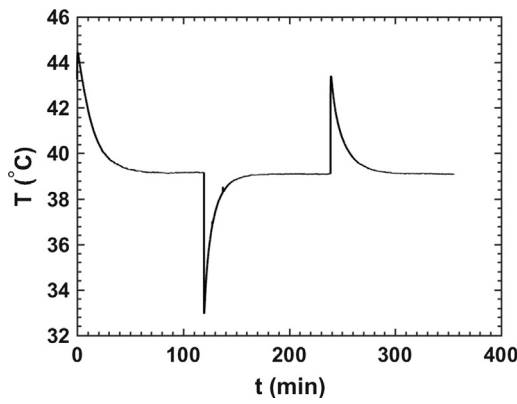


Fig. 9. Variation of sorbent temperature with time, data collected in our G-LPJ test bed.

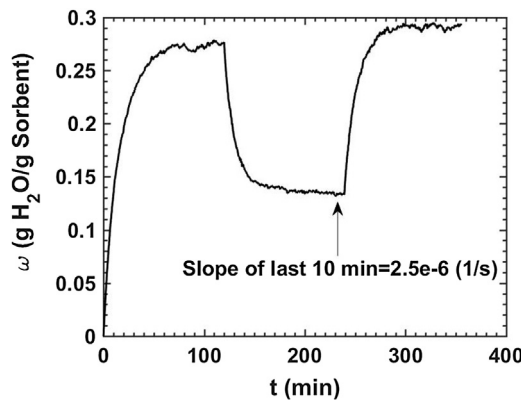


Fig. 10. Variation of water uptake with time, data collected in our G-LPJ test bed.

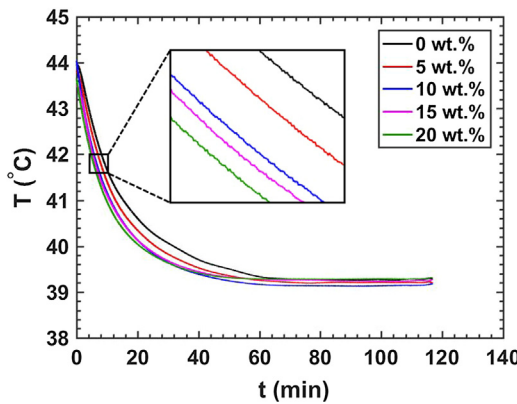


Fig. 11. Variation of average sorbent temperature versus time for various graphite flake contents, data collected in our G-LPJ test bed.

nature of de/adsorption processes, respectively. After this temperature drop/jump, the sorbent is heated up/cooled down to continue the de/adsorption processes. The rate of these heat up/cool down processes after the temperature drop/jump takes place determines the performance of sorption cooling systems. Fig. 10 also depicts the de/adsorption processes as the vapour is de/adsorbed by the sorbent material. It is noted that during the first sorption process, the temperature jump and the uptake are higher than the next sorption processes as the sorbent is vacuum dried before each test. Furthermore, Fig. 10 shows that the de/adsorption processes continued until the sorbent reached equilibrium condition based on the sorption rate ($d\omega/dt$) for the last 10 min. The results presented in the following sections are the de/

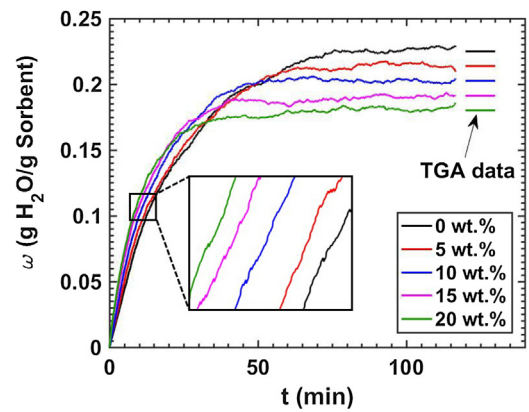


Fig. 12. Variation of water uptake versus time for various graphite flake content composites (data collected in our G-LPJ test bed).

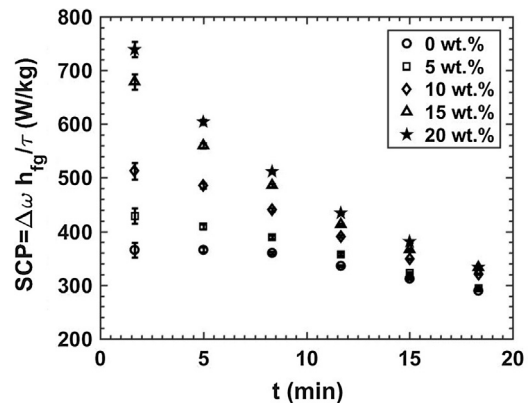


Fig. 13. Variation of specific cooling power versus sorption time for various graphite flake contents.

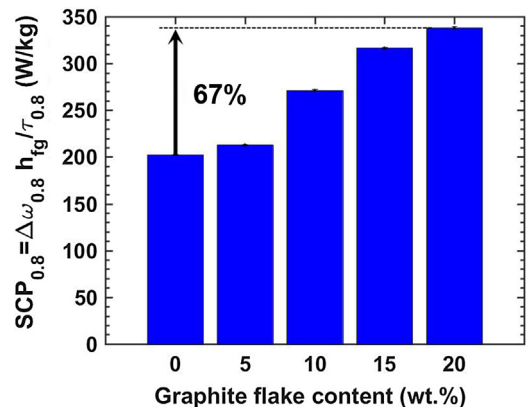


Fig. 14. Variation of $SCP_{0.8}$ versus graphite flake contents.

adsorption processes after the first sorption process.

3.1. Effect of graphite flake on heat transfer

It has been demonstrated in our previous studies [11,12] that the rate of heat removal from the sorbent, where the heat is generated, determines the performance of sorption cooling systems. In addition, it was shown that sorbent thermal diffusivity was the main limiting factor in the heat transfer from the sorbent to the heat transfer fluid through the heat exchanger.

Fig. 11 shows the variation of the average sorbent temperature versus time for different graphite flake contents. The sorbent

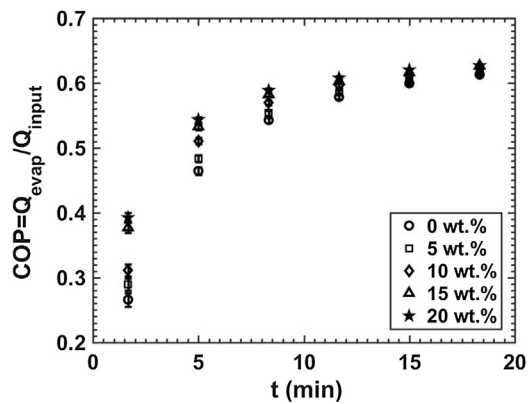


Fig. 15. Variation of COP versus sorption time for various graphite flake contents.

temperature was measured five times and a standard deviation of 0.1 °C was observed. One can see that the sorbent temperature decreases more rapidly for samples with greater graphite flake content. The maximum temperature reduction from samples with 0 wt% graphite flakes to the one with 20 wt% graphite flakes is 0.8 °C. One reason is that by adding graphite flakes, the sorbent thermal diffusivity increases, which enhances the heat transfer from the sorbent to the HEX, see Fig. 2. Furthermore, the heat generation decreases for samples with larger graphite flake content as they have less active material.

3.2. Effect of graphite flake on sorbate uptake

Fig. 12 shows the variation of water uptake with time for various graphite flake contents. As shown in Fig. 12, the equilibrium uptakes, measured with the G-LPJ test bed, are in good agreement with our TGA equilibrium data. Moreover, as can be seen, in the early stages of sorption, i.e. the first 20 min, the water uptake increases by increasing the graphite flakes content. The maximum uptake enhancement from samples with 0 wt% graphite flakes to the one with 20 wt% graphite flakes is 0.0325 g H₂O/g dry sorbent. The reason for this trend is that during this period, the heat generation rate in the sorbent is high. Hence, there is a higher need for enhanced sorbent thermal diffusivity; thus, increasing the graphite flake enhances the uptake performance. However, as the sorbent approaches saturation, the trend starts to reverse, which means that the uptake increases with a decrease of graphite content. That is because: as the sorbent approaches equilibrium, the heat generation rate reduces. As a result, the need for enhanced heat transfer decreases. Consequently, the sorbent with higher active material can uptake more, which leads to higher performance.

3.3. Effect of graphite flake on SCP

Fig. 13 shows the experimental SCP data collected in our G-LPJ test bed for various sorption times and different graphite flake contents. It can be seen that adding graphite flake enhances the SCP because the sorbent thermal diffusivity increases. Furthermore, it can be observed that by reducing the sorption time, the SCP enhancement due to adding graphite flake, increases because the heat generation rate increases. In addition, it is shown that adding 15 wt% graphite flakes or more, results in a significant increase in SCP for shorter sorption times. The reason can be attributed to a higher overall thermal diffusivity associated with adding graphite flakes for composites with more than 10 wt% additives, see Fig. 2.

An alternative, and more practical specific cooling power was proposed by Aristov et al. [34] to be calculated when the uptake reaches 80% of the equilibrium, Eq. (10):

$$SCP_{0.8} = \frac{\Delta\omega_{0.8} h_{fg@T_{evap}}}{\tau_{0.8}} \quad (10)$$

Fig. 14 shows the effect of graphite flake on SCP_{0.8}. It can be observed that SCP_{0.8} increases with the increase of graphite flakes content because the heat transfer rate increases, thereby reducing the time required for the sorbent to reach equilibrium. For example, composite sorbent containing 20 wt% graphite flake has 67% greater SCP_{0.8} than the composite sorbent with no thermally conductive additive.

3.4. Effect of graphite flake on COP

Fig. 15 shows the variation of coefficient of performance (COP) with time for different graphite flakes contents. It can be seen that COP increases by increasing the graphite flakes content as the sorbent thermal diffusivity and sorbate uptake increase; thus, evaporative cooling energy increases.

4. Conclusions

The effect of adding graphite flakes on the SCP and COP of sorption cooling systems was studied using a custom-built G-LPJ test bed. It was found that in the early stages of sorption, the sorber bed performance was notably improved (SCP from 365 to 604 W/kg and COP from 0.46 to 0.54 for 5 min sorption time) by adding graphite flakes due to the enhanced sorbent thermal diffusivity (from 0.23 to 1.38 mm²/s). Also, it has been shown that as the sorption rate reduces with time, the need for heat transfer enhancement, i.e. graphite flake additive, decreases. Therefore, a graphite flake content exists to achieve an optimum SCP and COP, which will be investigated in our future study.

Acknowledgement

The first author thanks the LAEC members, Dr. Claire McCague, postdoctoral fellow, and Dr. Wendell Huttema, lab engineer, for their assistance in building G-LPJ test bed and preparing sorbent materials required to run the experiments. The authors gratefully acknowledge the financial support of the Natural Sciences and Engineering Research Council of Canada (NSERC) through the Automotive Partnership Canada Grant No. APCPJ 401826-10. The SEM studies were conducted in the Simon Fraser University 4D Labs facility with the assistance of the technical staff. 4D LABS shared facilities are supported by the Canada Foundation for Innovation (CFI), British Columbia Knowledge Development Fund (BCKDF), Western Economic Diversification Canada (WD), and Simon Fraser University (SFU).

References

- [1] Building Energy Data Book, U.S. Department of Energy, 2012.
- [2] A.A. Askalany, M. Salem, I.M. Ismael, A.H.H. Ali, M.G. Morsy, B.B. Saha, An overview on adsorption pairs for cooling, *Renew. Sustain. Energy Rev.* 19 (2013) 565–572.
- [3] W. Pridasawas, Solar-driven refrigeration systems with focus on the ejector cycle, 2006.
- [4] V. Johnson, Fuel used for vehicle air conditioning: a state-by-state thermal comfort-based approach, SAE Pap., 2002.
- [5] R. Wang, R. Oliveira, Adsorption refrigeration—An efficient way to make good use of waste heat and solar energy, *Prog. Energy Combust. Sci.* 32 (4) (2006) 424–458.
- [6] A. Sharafian, M. Bahrami, Adsorbate uptake and mass diffusivity of working pairs in adsorption cooling systems, *Int. J. Heat Mass Transf.* 59 (1) (2013) 262–271.
- [7] R. Farrington, J. Rugh, Impact of vehicle air-conditioning on fuel economy, tailpipe emissions, and electric vehicle range, in: *Proceeding of the Earth Technologies Forum*, 2000.
- [8] W. Wu, H. Zhang, D. Sun, Mathematical simulation and experimental study of a modified zeolite 13X–water adsorption refrigeration module, *Appl. Therm. Eng.* 29 (2009) 645–651.
- [9] Y. Zhao, E. Hu, A. Blazewicz, Dynamic modelling of an activated carbon–methanol adsorption refrigeration tube with considerations of interfacial convection and transient pressure process, *Appl. Energy* 95 (2012) 276–284.
- [10] A. Sharafian, C. McCague, M. Bahrami, Impact of fin spacing on temperature distribution in adsorption cooling system for vehicle A/C applications, *Int. J. Refrig.* 51

- (2015) 135–143.
- [11] H. Bahrehmand, M. Ahmadi, M. Bahrami, Analytical modeling of oscillatory heat transfer in coated sorption beds, *Int. J. Heat Mass Transf.* 121 (2018) 1–9.
- [12] H. Bahrehmand, M. Ahmadi, M. Bahrami, Oscillatory heat transfer in coated sorber beds: an analytical solution, *Int. J. Refrig.* (2018).
- [13] K.C. Chan, C.Y.H. Chao, A theoretical model on the effective stagnant thermal conductivity of an adsorbent embedded with a highly thermal conductive material, *Int. J. Heat Mass Transf.* 65 (2013) 863–872.
- [14] A. Rezk, R.K. Al-Dadah, S. Mahmoud, A. Elsayed, Effects of contact resistance and metal additives in finned-tube adsorbent beds on the performance of silica gel/water adsorption chiller, *Appl. Therm. Eng.* 53 (2) (2013) 278–284.
- [15] S. Yang, H. Kim, S. Narayanan, I.S. McKay, Dimensionality effects of carbon-based thermal additives for microporous adsorbents, *Mater. Des.* 85 (2015) 520–526.
- [16] L. Pino, Y. Aristov, G. Cacciola, G. Restuccia, Composite materials based on zeolite 4A for adsorption heat pumps, *Adsorption* 3 (1997) 33–40.
- [17] H. Demir, M. Mobedi, S. Ulku, The use of metal piece additives to enhance heat transfer rate through an unconsolidated adsorbent bed, *Int. J. Refrig.* 33 (2010) 714–720.
- [18] A.A. Askalany, S.K. Henninger, M. Ghazy, B.B. Saha, Effect of improving thermal conductivity of the adsorbent on performance of adsorption cooling system, *Appl. Therm. Eng.* 110 (2017) 695–702.
- [19] L.F. Cabeza, A. Sole, C. Barreneche, Review on sorption materials and technologies for heat pumps and thermal energy storage, *Renew. Energy* 110 (2017) 3–39.
- [20] D. Aydin, S.P. Casey, S. Riffat, The latest advancements on thermochemical heat storage systems, *Renew. Sustain. Energy Rev.* 41 (2015) 356–367.
- [21] S. Mauran, P. Parades, F. L'haridon, Heat and mass transfer in consolidated reacting beds for thermochemical systems, *Heat Recover. Syst.* 13 (1993) 315–319.
- [22] A. Sharafian, M. Bahrami, Assessment of adsorber bed designs in waste-heat driven adsorption cooling systems for vehicle air conditioning and refrigeration, *Renew. Sustain. Energy Rev.* 30 (2014) 440–451.
- [23] J.J. Guilleminot, J.B. Chalfen, A. Choisier, “Heat and Mass Transfer Characteristics of Composites for Adsorption Heat Pumps”, International Adsorption Heat Pump Conference, AES 31, ASME, New York, 1993.
- [24] K. Wang, J.Y. Wu, R.Z. Wang, L.W. Wang, Effective thermal conductivity of expanded graphite-CaCl₂ composite adsorbent for chemical adsorption chillers, *Energy Convers. Manag.* 47 (13–14) (2006) 1902–1912.
- [25] K. Fayazmanesh, C. McCague, M. Bahrami, Consolidated adsorbent containing graphite flakes for heat-driven water sorption cooling systems, *Appl. Therm. Eng.* 123 (2017) 753–760.
- [26] T. Eun, H. Song, J. Hun Han, K. Lee, J. Kim, Enhancement of heat and mass transfer in silica-expanded graphite composite blocks for adsorption heat pumps: Part I. Characterization of the composite blocks: Amélioration du transfert de chaleur de blocs en matériaux composite graphite-silice expansé/d, *Int. J. Refrig.* 23 (1) (2000) 64–73.
- [27] X. Zheng, L.W. Wang, R.Z. Wang, T.S. Ge, T.F. Ishugah, Thermal conductivity, pore structure and adsorption performance of compact composite silica gel, *Int. J. Heat Mass Transf.* 68 (2014) 435–443.
- [28] ISO22007-2, lastics-determination of thermal conductivity and thermal diffusivity-part 2: transient plane heat source (hot disc) method, 2008.
- [29] M. Khajepour, C. McCague, S. Shokoya, M. Bahrami, Effect of Conductive Additives on Performance of CaCl₂-Silica Gel Sorbent Materials, in: Heat Power Cycles conference, 2018.
- [30] S. Kirkpatrick, Percolation and conduction, *Rev. Mod. Phys.* 45 (4) (1973).
- [31] B. Ghanbarian, H. Daigle, Thermal conductivity in porous media: percolation-based effective-medium approximation, *Water Resour. Res.* 52 (2016) 295–314.
- [32] R.E. Critoph, Simulation of a continuous multiple-bed regenerative adsorption cycle, *Int. J. Refrig.* 24 (5) (2001) 428–437.
- [33] R.J. Moffat, Describing the uncertainties in experimental results, *Exp. Therm. Fluid Sci.* 1 (1988) 3–17.
- [34] Y.I. Aristov, I.S. Glaznev, I.S. Girmik, Optimization of adsorption dynamics in adsorptive chillers: loose grains configuration, *Energy* 46 (1) (2012) 484–492.